RSC Advances

Synthesis and characterization of pH-responsive nanohydrogels as biocompatible drug carriers based on chemically modified Tragacanth Gum polysaccharide

Khadijeh Hemmati, Arameh Masoumi, Mousa Ghaemy*

Polymer Research Laboratory, Faculty of Chemistry, University of Mazandaran, Babolsar, Iran

*Corresponding author, E-mail address: ghaemy@umz.ac.ir; Tel/Fax: +98-112-35302353

ABSTRACT

In this work, the preparation of pH-responsive nanohydrogels based on Tragacanth gum (TG) polysaccharide and glycidyl methacrylate (GMA) was investigated. Ring opening of epoxide group of GMA by hydroxyl groups of TG led to preparation of TG-GMA which was then transformed to cross-linked nanohydrogel network (TG-MA) via radical polymerization using $K_2S_2O_8$ as initiator. The obtained nanohydrogels were characterized using techniques such as FT-IR, ^{1}H NMR, scanning electron microscope (SEM), zeta sizer and thermogravimetric analysis (TGA). The gel content of nanohydrogels showed dependence on the weight ratio of TG/GMA. According to the results, the swelling behavior of the prepared TG-MA nanohydrogels showed significant dependence on the gel content, pH, and immersion time. The loading and *in vitro* release of Quercetin as a model drug was investigated at pH 7.0. The obtained results showed that the rate of drug release depends on the swelling of nanohydrogels and cross-linker content. Furthermore, the investigation shows that pH-responsive TG-MA nanohydrogels can be a good candidate for further tests as drug carriers.

Keywords: Tragacanth Gum, biocompatible, nanohydrogel, drug delivery, Quercetin.

Introduction

Hydrogels have gained considerable interest as drug containers or release rate controlling barriers among various kinds of polymeric systems.[1-8] Hydrogels are polymer networks that have a high number of hydrophilic groups or domains and are prevented from dissolving due to the chemical or physical bonds formed between the polymer chains. They can also control drug release by changing the gel structure in response to environmental stimuli, such as pH, temperature, ionic strength, and electric field.[3, 9, 10] Moreover, hydrogels have several additive characteristics that make them excellent drug delivery vehicles: (1) They are convenient, biocompatible, and stable drug delivery systems for molecules as small as non-steroidal anti-inflammatory drugs (NSAIDs) or as large as proteins and peptides,[11] (2) many polymers used in hydrogel preparations such as PAA, PHEMA, PEG, and PVA with mucoadhesive and bioadhesive characteristics enhance drug residence time and tissue permeability,[12, 13] and (3) the adhesive property can help enhance site-specific binding to specific regions, such as the colon, nose, and vagina.[14] Due to physio-chemistry similarity (both compositionally and mechanically) between hydrogels and native extracellular matrix, hydrogels can also serve as dual-propose devices, acting as a supporting material for cells during tissue regeneration as well as delivering a drug payload.[15, 16] Several natural polymers such as those found in diet, due to this fact that they are more available and more susceptible to microbial biodegradation, are preferred over synthetic materials for colonic drug delivery.[17] Natural gum polysaccharides have also attracted interest in the field of drug delivery due to their outstanding merits, such as being abundant, cheap, biodegradable and safe characteristics. However, there are certain problems with the polysaccharides such as pH dependent solubility, uncontrolled rates of hydration, thickening and drop in viscosity on storage, and the possibility of microbial contamination. These drawbacks can be minimized by chemical modifications such as grafting or crosslinking of vinyl monomers onto polysaccharides which

enables their use for specific drug delivery purposes.[18-21] Natural hydrophilic tragacanth gum (TG) with unique physical, chemical and also biological properties such as non-toxicity, stability over wide pH range, biocompatibility, eco-friendliness and safety for oral intake can be introduced as a future device for biomedical applications and tissue engineering.[22,23] The primary and secondary hydroxyl and carboxylic acid groups present in TG molecules provide positions for acting as crosslinking reagent and also intermolecular hydrogen bonding with other materials bearing hydroxyl, carboxylic acid, amine, and aldehyde groups.[18, 24]

Quercetin (3,3,4,5,7-pentahydroxyflavone), a potent anticancer drug, is a dietary flavonoid present in vegetables, fruits, seeds, nuts, tea, and red wine with potential chemoprotective effects. The main limitation of quercetin is its poor solubility in water and instability in physiological medium which restricts the use of this flavonoid to oral administration. Several attempts were made by different researchers to increase the bioavailability of quercetin.[(25-27)] However, no attempts have been made for increasing the oral bioavailability of quercetin by incorporating the drug in the matrix of biopolymer like TG which on the other hand promises the drug delivery to a higher intestinal pH in which the drug is soluble enough.

The main objective of this study was to develop an alternative procedure for the preparation of nanohydrogels based on the functionalized Tragacanth gum (TG) for acting as a polymeric drug carrier. The preparation of nanohydrogels includes synthesis of methacrylate-functionalized TG (TG-GMA) by reaction of TG with Glycidyl methacrylate (GMA) in a basic aqueous solution. Then, the nanohydrogels (TG-MA) were prepared by free radical polymerization of TG-GMA using aqueous solution of potassium persulfate as radical initiator. The prepared nanohydrogels were fully characterized by FT-IR, SEM, and zeta sizer and their properties such as thermal, gel percent and swelling behavior were investigated. The gel content of nanohydrogels were investigated by changing the weight ratio of TG/GMA, and the swelling behavior showed dependence on the gel content, medium pH, and

immersion time. Herein, quercetin was used as the model drug and was encapsulated into the nanohydrogels using swelling-diffusion method. In *vitro* Quercetin release behavior was investigated for different hydrogels at pH 7.

Experimental

Materials

The high quality Iranian Tragacanth Gum (TG) was purchased from local pharmaceutical shop. Glycidyl methacrylate (GMA, Acros Organics), triethylamine (TEA, Fluka), potassium persulphate (Sigma) were of analytical grade and used without purification, except for di dichloromethane (DCM) which was distilled before use.

Chemical modification of TG

TG was sieved to remove dust and small particles, purified with ethanol extraction and then dried under vacuum for 48 h and kept in desiccators before use. As listed in **Table 1**, four series of modified TG were synthesized by changing the weight ratio of TG/GMA. A typical procedure for preparation of modified TG is given below. In the first step in a round-bottom flask equipped with a nitrogen inlet and a magnetic stirrer, 0.5 g clean fine powder TG was dispersed in distilled water (50 mL) and stirred for 1 h to attain homogenous mixture. Afterwards, TEA (0.02 mL) and GMA (1 mL) were added. A continuous supply of nitrogen was maintained throughout the reaction period. The resulting mixture was stirred for 72 h at 50 ^{0}C. The modified polysaccharide, labeled TG-GMA, was purified by precipitation in acetone and remixed in water. To remove unreacted residues, prior to being dried under reduced pressure, this cycle was repeated at least three times.

Nanohydrogel synthesis

In order to obtain nanohydrogel, 0.36 g TG-GMA was dissolved in deionized water. Then, 10 mL of aqueous solution of potassium persulfate (0.05 g) was added and the mixture was stirred for 15 min at room temperature and then, heated to 70 $^{\circ}$C and stirred for 30 min. The solid product, after separation by filtration was washed several times with distilled water to remove the remaining materials and dried in a vacuum oven at 60 $^{\circ}$C.

Gel fraction

Freshly prepared nanohydrogels were dried in an oven at 50 ^{0}C to a constant weight (W_0). Then, to remove the sol fraction, nanohydrogels were immersed in deionized water and every 8 h for 72 h, the water was renewed, after which the hydrogels were dried to a constant weight (W_g). The gel fraction percent was calculated using Eq. (1).

$$Gel\ fraction\% = (W_g/W_0) \times 100 \qquad (1)$$

Table 1. Starting materials in the preparation of nanohydrogels and gel fraction of them.

Formulation	Code	TG (g)	GMA (g)	$K_2S_2O_8$ (g)	Gel Fraction(%)
	TG-MA1	0.5	0.25	0.05	42
	TG-MA2	0.5	0.5	0.05	64
TG-MA	TG-MA3	0.5	0.75	0.05	91
	TG-MA4	0.5	1	0.05	94

Swelling studies

The swelling behavior of TG-MA nanohydrogels was determined as a function of ionic strength, pH, and immersion time. Sodium chloride solutions in concentrations ranging from 0.01 to 0.25 mg mL^{-1} were prepared to investigate the dependence of water uptake (Wu) on

ionic strength. The dependence of Wu on pH was determined by using PBS with pH ranging from 2 to 10 at 37 ^{0}C. Also dependence of Wu on time was determined by changing the contact time from 1h to 10 h. The Wu values were estimated from the following equation:

$$Wu = \frac{W_S}{W_d} \qquad (2)$$

where W_S is the weight of the nanohydrogel swollen to equilibrium at different conditions and W_d is the weight of the dried nanohydrogel. To check reproducibility, swelling experiments were repeated at least four times.

In vitro drug loading and release

The hydrophobic Quercetin as a model drug was loaded into the TG-MA3 and TG-MA4 nanohydrogels by the swelling-diffusion method. A certain amount of the dried nanohydrogel was allowed to swell in the drug solution (25 mL) of different concentrations at room temperature. After interval time, the nanohydrogel was removed from the solution and placed in 20 mL buffer solution and stirred vigorously for 48 h to extract drug from the hydrogel. Then they were dried to a constant weight in a vacuum oven at 45 ^{0}C. The remaining solution was diluted to 50 mL, filtered, and assayed by UV-vis spectrophotometer at 256 nm. The nanohydrogel drug-loading content (DL) and drug entrapment efficiency (EE) were calculated using Eqns. (3 and (4), respectively.

$$\text{Encapsulation efficiency (\%)} = \frac{Actual\ loading}{Theoritical\ loading} \times 100 \qquad (3)$$

$$\text{Drug loading (\%)} = \frac{Weight\ of\ drug\ in\ the\ hydrogel}{Weight\ of\ the\ hydrogel} \times 100 \qquad (4)$$

In *vitro* release studies of Quercetin from nanoparticles were studied using several beakers each containing 100 mL PBS at pH 7, incubated at 37±0.1 ^{0}C under constant shaking at 100 rpm. At regular time intervals 3 mL release medium was withdrawn from each beaker and

replaced with 3 mL of fresh PBS to keep constant volume, then the concentration of Quercetin in the medium was analyzed by UV -vis spectrophotometer at 256 nm.

Characterization

FT-IR spectra were recorded on KBr pellets using a Bruker Tensor 27 spectrometer (Bruker, karlsrohe, Germany). ^{1}H NMR spectra of TG, TG-GMA and GMA were recorded on a 400 MHz Bruker Advance DRX instrument. Deionized water for TG and TG-GMA and CD_3Cl for GMA were used as solvents and tetramethyl silane as an internal standard. The thermogravimetric analysis (TGA) was carried out on a Polymer Laboratories (PL) thermal gravimetric analyzer (TGA) from the ambient temperature to 800 [0]C under nitrogen atmosphere at the heating rate of 10 [0]C/min. Mean diameter of all nanoparticles were determined using a zeta sizer (Nano ZS, Malvern Instrument, UK) at 25 [0]C. To investigate surface morphology of the nanohydrogels, scanning electron microscopy (SEM) (Model: Hitachi S4160) was employed. A fragment of the dried samples was mounted on a SEM sample mount and was sputter coated with gold for 2 min, and then was mounted in SEM and scanned at the desired magnification. APHS-3C pH-meter (Shanghai, Tianyou) was used for pH measurements.

Titration and back titration analyses of TG and TG-MA nanohydrogels

To define the molar concentration of COOH groups in both the initial TG polymer and the final TG-MA nanohydrogels, titration and back titration analyses were used, respectively. The mmol of COOH groups in 1 g of TG was measured by titration. 1g TG was dissolved in 100 mL distilled water and then COOH groups of TG were neutralized by addition NaOH solution (1 M) to the equivalence point of titration. For the nanohydrogel which is not soluble in water, back titration was used to determine the COOH groups. Aqueous solution of TG-MA (1 g in 100 mL distilled water) was adjusted to pH 9 with 1 M NaOH at room temperature, stirred for 8 h. The excess amount of base was neutralized by addition of HCl

solution (1 M) to the equivalence point of titration. The results showed that the number of the

COOH groups in TG and TG-MA were 50 mol and 47 mol in 1g samples, respectively.
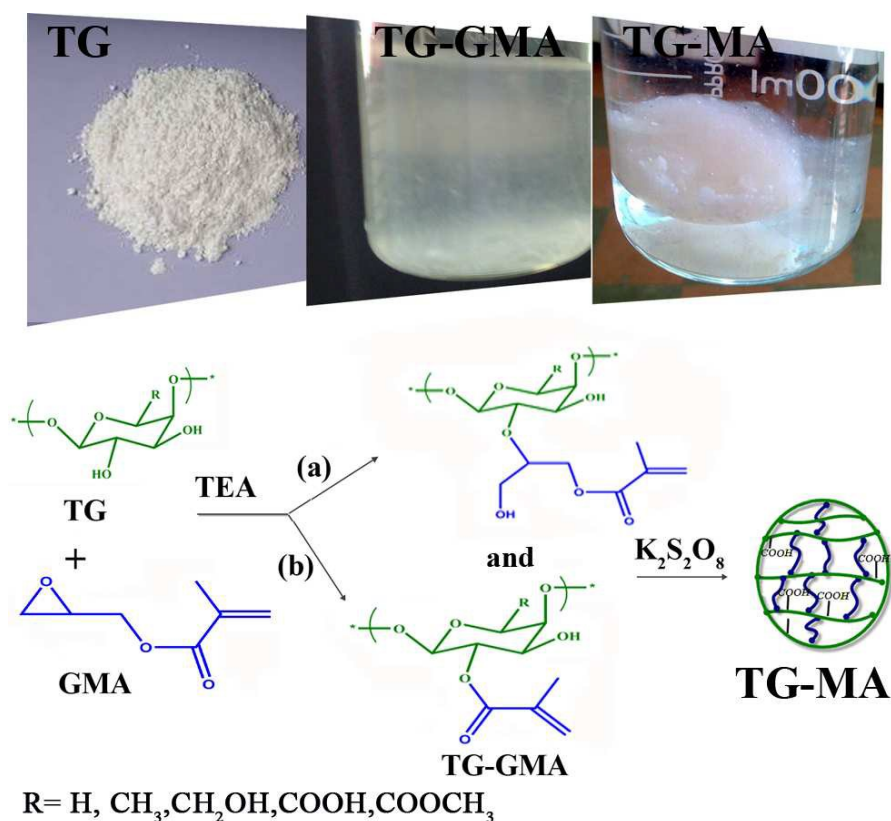
Fig. 1. Illustration of synthetic procedure for preparation of TG-MA nanohydrogels.

Results and discussion

Synthesis and characterization of nanohydrogels

As shown in **Fig. 1** and as reported by other researchers for their tested materials, [28, 29] it is

supposed that chemical modification of TG with GMA can occur through two pathways: (a)

by opening the epoxy ring, therefore whole GMA molecules are coupled to the

polysaccharide structure, and (b) by transesterification reaction so that the methacrylate

molecule is coupled to the polysaccharide structure and glycidol is formed as a byproduct.

The GMA modified TG at this stage is designated as TG-GMA. Different weight ratios of

GMA: TG was used, as listed in **Table 1**. The purpose of this work was to incorporate vinyl groups of GMA into the TG structure to form nanohydrogels not to verify whether transestereification and/or epoxy ring opening occur.
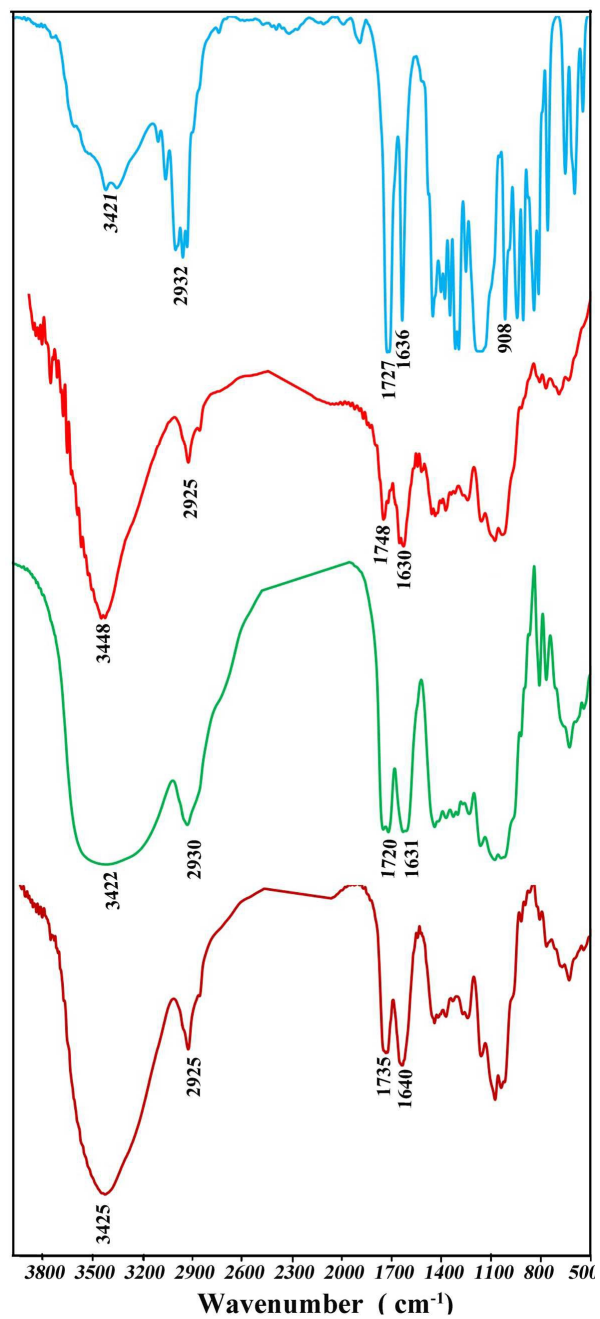
Fig. 2. FT-IR spectra of GMA (a), TG (b), TG-GMA (c), and TG-MA nanohydrogel (d).

Fig. 2 (a-d) shows the FT-IR spectra of GMA, TG, TG-GMA and TG-MA hydrogel. The spectrum of GMA in **Fig. 2(a)** shows C=O stretching at 1727 cm^{-1}, C=C stretching at 1636 cm^{-1}, epoxide stretching at 908 cm^{-1}, and C–H stretching at 2932 cm^{-1}.[30] **Fig. 2(b)** shows FT-IR spectrum of TG. The absorption bands at 1748 and 1630 cm^{-1} in TG spectrum are related to stretching vibrations of C=O groups of ester and carboxylic acid, respectively. Absorption band at 1100-1200 cm^{-1} is related to vibration of C–O bond. FT-IR spectrum of TG-GMA is shown in **Fig. 2(c).** The sharp absorption band of the epoxide ring at 908 cm^{-1} has been replaced by a wide absorption band of C–O bond indicating the opening of epoxide ring. There are two absorption bands at 1720 cm^{-1} and 1631 cm^{-1} which can be related to C=O vibration stretching of ester and carboxylic acid groups which have probably been overlapped with C=C absorption band of methacrylate. FT-IR spectrum of TG-MA nanohydrogel is much similar to the spectrum of TG-GMA showing that the nanohydrogel contains OH and C=O groups of TG and GMA in the structure.

TG-GMA/$K_2S_2O_8$ solutions in deionized water were heated at 70 ºC with stirring for 30 min to prepare chemically cross-linked network of nanohydrogels, as shown in **Fig. 1** and designated as TG-MA. The characterization of TG-MA nanohydrogel by FT-IR as shown in **Fig. 2d** indicates shifting of the C=O stretching band from 1720 to 1735 cm^{-1} due to cross-linking reaction involving –C=C – of the methacrylate unit. Also, the absorption band at 1651 cm^{-1} related to the C=O group of carboxylic acid confirms that –COOH groups in TG backbone remained intact after preparation of TG-GMA. After the cross-linking reaction, due to the loss of conjugation of the ester groups, the C=O stretching band shifted from 1720 to 1735 cm^{-1}, which indicated the occurrence of the cross-linking reaction.[17,18] The modification of TG with GMA was also confirmed by ^{1}H-NMR analysis. **Fig. 3** shows the ^{1}H-NMR spectra of GMA, TG, and TG-GMA. As presented in ^{1}H-NMR spectrum of TG-GMA, the

signals at 6.16 and 5.81 ppm were attributed to the vinyl hydrogen originally present in

GMA.
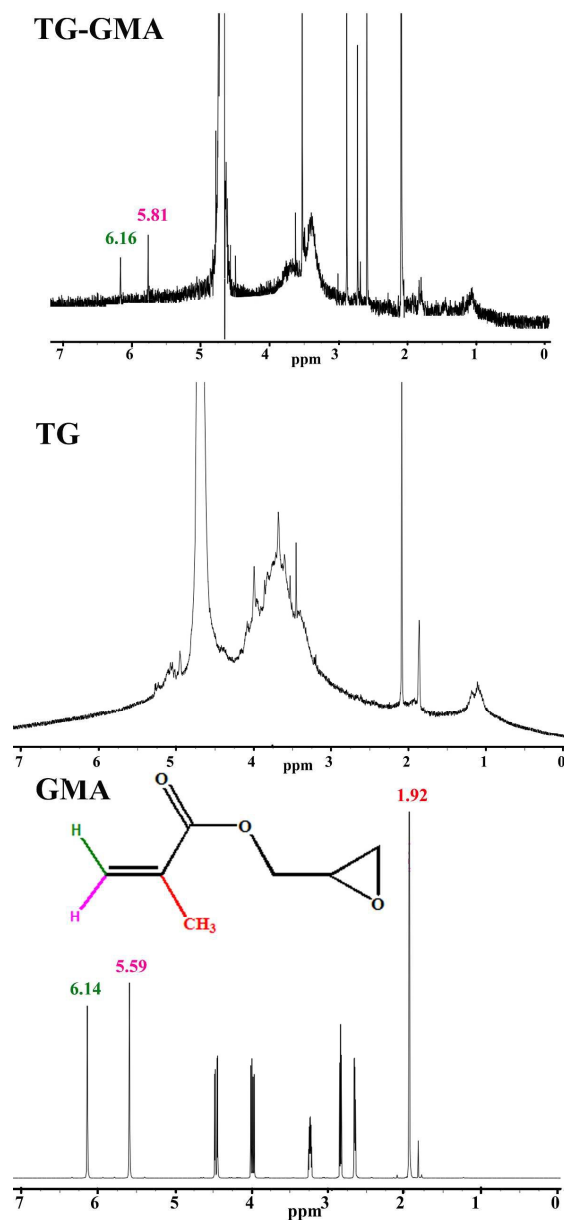
Fig. 3. ^{1}H-NMR spectra of TG and TG-GMA were recorded in D$_2$O and spectrum of GMA in

CDCl$_3$.

SEM analysis

The SEM images of surface morphology of the nanohydrogels are observed in **Fig. 4(a-c)**.

Figs. 4(a) and (**b**) show SEM images of dried surface of TG-MA3 hydrogel at two different

scales. The SEM images of TG-MA hydrogel exhibits a highly macroporous sponge like structure while SEM image of TG in panel **c** shows a tight structure. The pores that became visible on the surface of TG-MA3 nanohydrogel were attributed to solvent evaporation.
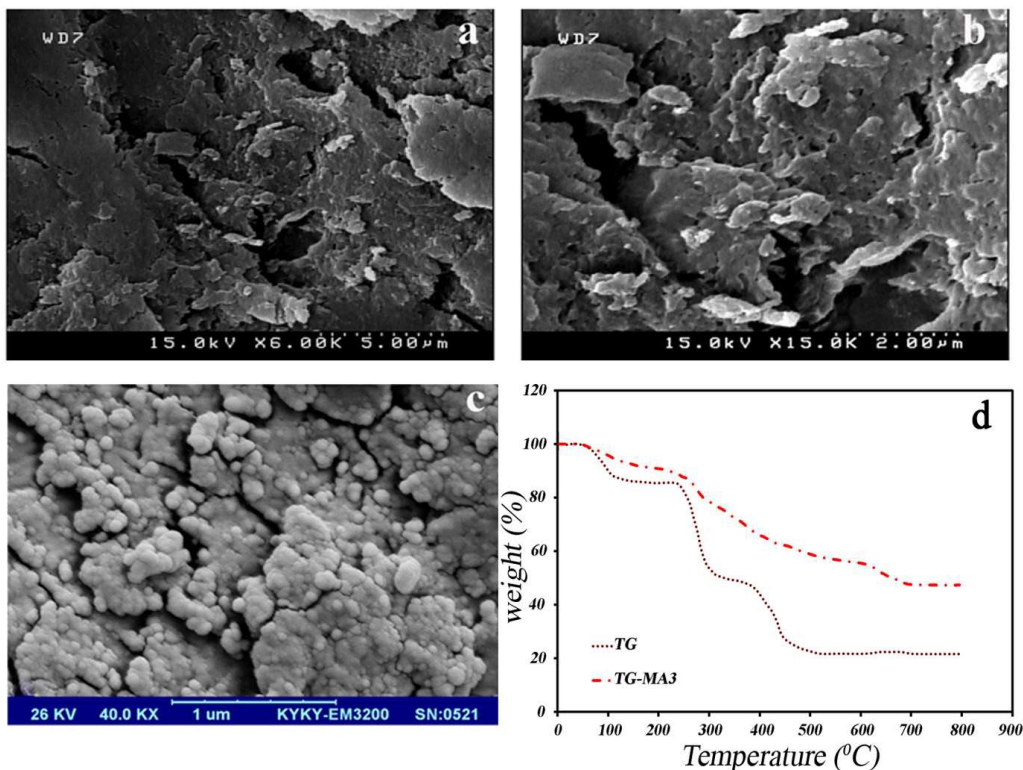
Fig. 4. SEM images of dried surface of TG-MA3 sample (panels **a** and **b)** at two different scales, panel **c** is the image of dry neat TG, and panel **d** shows TGA curves of TG and TG-MA3 hydrogel.

Thermal analysis

It is well known that thermal degradation of polysaccharides is quite complex and starts with depolymerization through random chain scission associated with degradation followed by molecular rearrangements. In general, decomposition of polysaccharides consists of four phases: desorption of physically absorbed water, removal of structural water (dehydration reactions), depolymerization and finally formation of polynuclear aromatic hydrocarbon.[31] **Fig. 4d** represents TGA curves of the TG and TG-MA3 nanohydrogel. According to these

curves, TG showed the initial weight loss of about 12 wt% at 100 ^{0}C due to evaporation of the absorbed humidity. This was followed by two-steps weight losses of about 36 wt% and 25 wt% at 240-310 ^{0}C and 400-500 °C, respectively. These weight losses can be related to decomposition of highly branched heterogeneous macromolecule consisting of water-soluble fraction and insoluble fraction. In case of TG-MA3, initial and final weight loss temperatures are observed at 100 ^{0}C and 700 ^{0}C, respectively. Three stages decomposition were observed for TG-MA3 nanogel network. The first stage loss of ~10 wt% at 100 ^{0}C is due to evaporation of absorbed water. The second stage weight loss of ~35 wt% in the range of 240-570 °C was followed by a third stage weight loss of ~8 wt% in the range of 580-710 °C can be due to decomposition of cross-linked network of highly branched heterogeneous TG with GMA. The char yield (residue) is ~47% for TG-MA3 and 20% for TG at 700-800 °C. The higher residue at the selected temperature, i.e. 800 °C, shows that cross-linked network TG-MA3 nanogel has higher thermal stability than neat TG. This can be pertained to the hard and rigid structure of cross-linked network compared to the flexible structure of TG. It is clear that the existence of cross-links in the network structure of TG-MA3 and chemical interactions between polymer chains shifted decomposition temperature towards higher temperatures indicating enhanced thermal stability of the nanohydrogel.

Gel fraction

The gel content of nanohydrogels as a function of varying the amounts of GMA is listed in **Table 1**. The gel content was obtained after a long time hot extraction with distilled water. The gel content in the nanohydrogels increased up to 94% with increasing the amount of GMA from 30 to 70 wt%. The increase in the gel percent is fast initially and becomes steady later due to formation of many cross-links restricting the polymer chains movement.

Effects of main factors on the water uptake ratio (W$_u$)

One of the most important factors that determine properties and applications of nanohydrogels is the capacity of swelling. The swelling of nanohydrogels is a function of the many structural factors such as pK$_a$ of the ionizable group, degree of ionization, cross-linking density, hydrophilicity and the properties of the swelling medium such as temperature, solution pH, contact time and ionic strength. Therefore, the effect of these factors on the water uptake of the prepared hydrogels is discussed below.
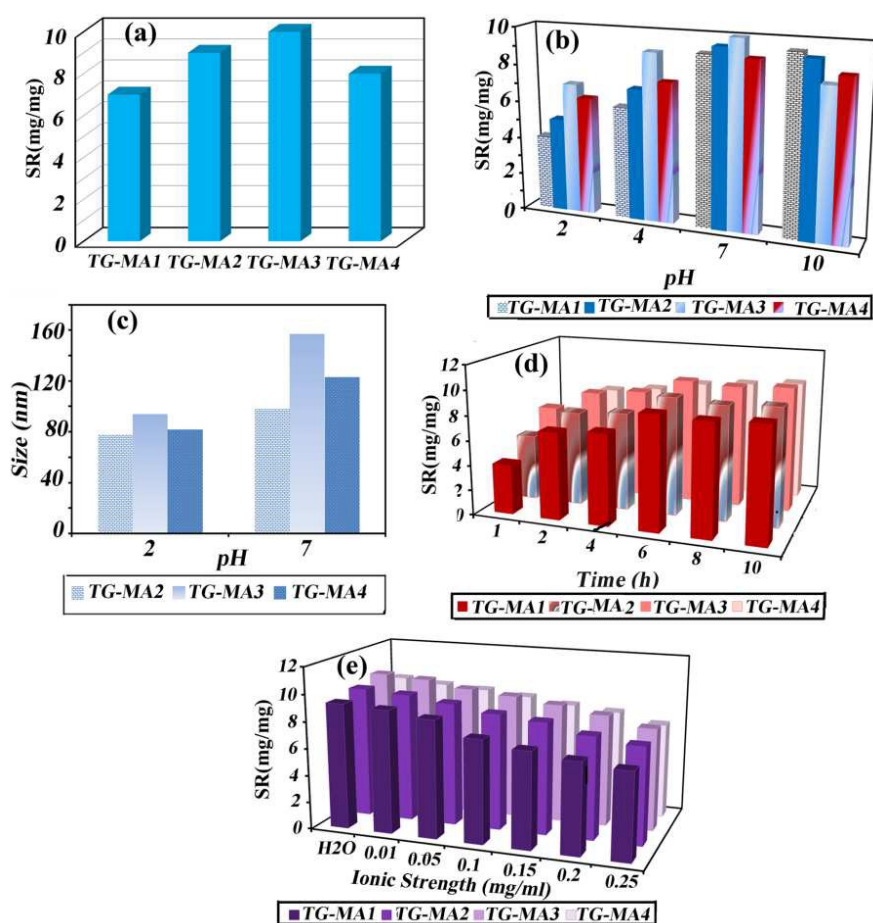
Fig. 5. The effect of cross-linker content (a), solution pH (2.0-10.0) (b), immersion time (1-10 h) (c), and ionic strength (0.01-0.25 mg mL^{-1})(d) on the water uptake ratio (conditions: at 25 ^{0}C, C$_0$ = 100 mg L^{-1}, ionic strength = 0.01mg mL^{-1}, pH 7, immersion time = 6 h, with varying the initial level of related factor).

14

Effect of cross-linking ratio

The cross-linking ratio is one of the most important factors that affect the swelling of nanohydrogels. Cross-linking hinders the mobility of the polymer chain, hence lowering the swelling ratio.[4, 13, 32] As can be seen in **Fig. 5a**, the swelling ratio (SR) continued to increase with increasing the amount of cross-linker. The results show that when the cross-linker GMA content is less than 0.75 g, the network formation is not complete and some TG which is not involved in the network formation dissolves during swelling process. Therefore, the measured swelling ratio (SR) values (mg/mg) and the gel content are low when the GMA amount is less than 0.75 g. However, when the GMA content is 0.75 g (TG-MA3), more networks is formed and the gel content increased to the highest value of 91 wt%. Also, the SR value of this nanohydrogel (TG-MA3) is the highest value of around 10 mg/mg. However, the SR value decreased when the amount of cross-linker, GMA, was more than 0.75 g. Highly cross-linked nanohydrogel sample of TG-MA4 prepared from 1 g GMA, has a tight network structure and swell less compared to more flexible network of TG-MA3.

Effect of solution pH

pH sensitive nanohydrogels play an important role in controlled drug delivery systems. Therefore, the swelling behavior of TG-MA nanohydrogels to the pH of external medium was investigated by varying the pH in the range of 2.0–10.0. **Fig. 5b** presents the water uptake (Wu) or swelling ratio (SR) profiles of the TG-MA nanohydrogels plotted against pH variation. It is evident that SR of the nanohydrogels showed a significant pH-dependence and has increased with increasing the surrounding pH value from 2 to 7. All nanohydrogels obtained their maximum swelling at pH 7. This observation can probably be attributed to this fact that the ionization of carboxylic acid groups in polymeric network generates electrostatic repulsion forces between the adjacent polymer chains. [33, 34] It was expected that the swelling ratio of the nanohydrogel reaches its maximum value at pH 10, but interaction of water

molecules with the acid molecules becomes restricted due to interaction between hydrogel and basic species in an alkaline environment. Therefore, the swelling ratio decreased obviously. Furthermore, the size of TG-MA2, TG-MA3 and TG-MA4 nanohydrogels particles was measured by DLS at pH 2 and 7, and the results are shown in **Fig. 5c**. The size of particles is less than 100 nm at pH 2 and increased with increasing pH upto 7, and this can also confirm the results obtained from the swelling tests at varying pH values. The size of the tested particles are in the range of nano at pH 2 (~80 nm) and increased to ~140 nm at pH 7. This pH-sensitivity suggests that these nanohydrogels can be used as a biological on–off switch for an intelligent drug delivery system triggered by the external pH change in a body.

Effect of time

The water uptake of nanohydrogels was monitored for a long time and the measurements were continued until a constant mass was reached for each hydrogel sample. As can be seen in **Fig. 4d**, the swelling capability of all investigated nanohydrogels increased with increasing the swelling time and reached the equilibrium value after 6 h of immersion. This behavior can be due to the fact that during the initial stages, a large number of vacant active sites are available for water molecules.

Effect of ionic strength

The swelling behavior of the nanohydrogels was investigated as a function of the ionic strength at pH 7. The results are shown in **Fig. 5e**. It is observed that the W_u of the nanohydrogel is significantly affected as the ionic strength of the surrounding liquid changes. The swelling ratio percentage of the nanohydrogels decreased as the ionic strength increased from 0.01 to 0.25 M. This effect can be attributed to the reduction of the concentration difference of mobile ions between the hydrogel and the solution, and also due to the decrease of the osmotic pressure inside the nanohydrogel, afterward, sharp decrease in the swelling degree of the nanohydrogel.[33, 35, 36]

Quercetin loading and encapsulation efficiency

To investigate the release behavior of a model drug from TG-MA3, Quercetin was incorporated into the nanohydrogels and entrapped efficiency was investigated as a function of time and initial drug concentration in PBS solution at pH 7 (**Fig. 6a** and **b). Fig. 6a** shows the effect of amount of cross-linker on the entrapped efficiency (EE) of Quercetin in the prepared nanohydrogels. The results showed that EE value was the highest for TG-MA3. This is because TG-MA3 has the highest swelling ratio at pH 7 and showed higher particle size than TG-MA4, as shown in Fig. 5(a-c). This suggests that the EE value was mainly dependent on the cross-linker GMA ratio and pore size of nanohydrogels. It can be concluded that when this ratio is optimum, as in the case of TG-MA3, there are suitable numbers of cross-links in the obtained network where Quercetin molecules accommodate inside the loops forming hydrogen bonding with the hydroxyl groups of TG. As can be seen in **Fig. 6b**, the EE value of Quercetin in TG-MA3 increased fast in the first 120 min and reached the maximum after in 150 min. As the dried nanohydrogel absorbed water, Quercetin molecules were transported with water due to the concentration gradient of Quercetin between outside and inside of the nanohydrogel. At the specific time, the encapsulation efficiency of Quercetin in the nanohydrogel increased with increasing the initial drug concentration and reached the maximum due to saturation which happened at high concentration. The particle size of the obtained blank (without drug) and drug loaded nanohydrogels were measured by DLS, and the results are shown in **Fig. 6c**. DLS measurements indicated that the average size of blank nanohydrogels, TG-MA4 and TG-MA3, were in the range of 120-155 nm at pH 7. As expected, the average size of these nanohydrogels increased to about 140 nm and 168 nm, respectively, after being loaded with Quercetin indicated that the drug was incorporated into the nanohydrogel effectively.
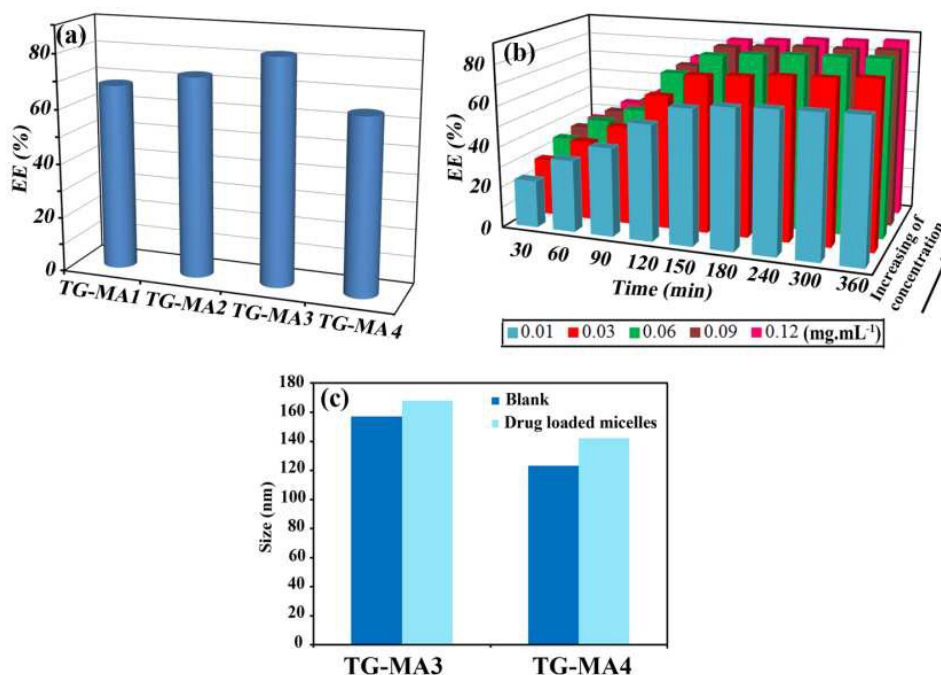
Fig. 6. (a) Effect of GMA content on EE, (b) effect of time on EE at various concentrations of quercetin in TG-MA3, and (c) size of TGMA3 and TGMA4 nanohydrogels before and after loading at pH 7.

In *vitro* release

Quercetin release was investigated by immersion of the drug loaded nanohydrogels in pH 7 buffer media up to 12 h. **Fig. 7(a)** displays the release profiles of nanohydrogels cross-linked with different amounts of GMA. As can be seen, the % cumulative release is low for the nanohydrogel cross-linked with 1g of GMA (TG-MA4). This can be due to the low swelling of nanohydrogel as a result of increasing the amount of GMA. In contrast, the high values of % cumulative release were observed for nanohydrogels with the optimum amount of GMA (TG-MA3). It is well known that drug release is attributed to three types of mechanisms: (1) release from the surface of particles, (2) diffusion through the swollen rubbery matrix, and (3) release due to structural erosion in the external environment.[23] As can be seen in **Fig. 7(a)**, both TG-MA nanohydrogels demonstrated similar release profiles. At the initial stage, high release rates were observed due to the dissolution of Quercetin molecules which were

attached loosely on the surface of nanohydrogels, the release occurred quickly to the surrounding medium. This shows the fact that the drug release from the swellable nanohydrogels is primarily controlled by the relatively high concentration gradient between the surrounding medium and the surface of nanohydrogels.[37] At the longer times, drug release becomes much slower because the drug release is controlled by diffusion rather than erosion of the matrix**.** As can be seen in Fig. 7, the drug release is the slowest for TG-MA4 nanohydrogels which can be due to the low amount of Quercetin molecules entrapped inside the loops of the network where large amount of GMA cross-linker was used. Furthermore, both formulations exhibited low amount of drug release in the simulated gastric conditions (pH 2), and high values in the simulated intestinal conditions (pH 7). It is clearly evident from these results that the release profile can be explained based on the pH influence on the structure of nanohydrogels. The release rate of Quercetin from nanohydrogels increased with increasing pH values, because in the basic medium the carboxylic acid groups dissociated and the repulsive force between the carboxyl anions swells the nanohydrogel enough to release drug expeditiously.

Mathematical model for predicting the drug release profile from nanohydrogels

Drug release from these nanohydrogels is treated as a partition phenomenon. The maximum cumulative release (%), α parameter, which is calculated from Eq. (5), expresses the physical chemical affinity of the drug between the nanohydrogel and solvent phases. With $\alpha > 0$, the diffusion of the drug between the nanohydrogel and the solvent phase is verified. This means that the processes of absorption and release of drug occur simultaneously.[38]

$$\alpha = C_{max}/1 - C_{max} \qquad (5)$$

Upon contact with the nanohydrogel, both the release and the absorption rates of the drug can be evaluated through changes of its concentration in solution. However, because the released drug can be reabsorbed by the nanohydrogel, its concentration in solution will be the

difference between the concentrations of drug released and absorbed. So reversible first-order kinetics (Eq. (6)) and reversible second-order release kinetics (Eq. (7)) were used to analyze the data obtained from the *in vitro* release studies to evaluate the kinetic models and release mechanism of drug from the systems described here. Fig. (7) shows the experimental data for drug released from (TG-MA3) and (TGMA4) nanohydrogels at pH 2 and t pH 7 as a function of time, plotted according to Eq. (6) (first-order kinetics, Fig. 7(b) and Eq. (7) (second-order kinetics, Fig. 7(c). The R^2 values, obtained from the linear regression analysis, for the reversible first-order and the reversible second-order release kinetics are summarized in **Table 2**.
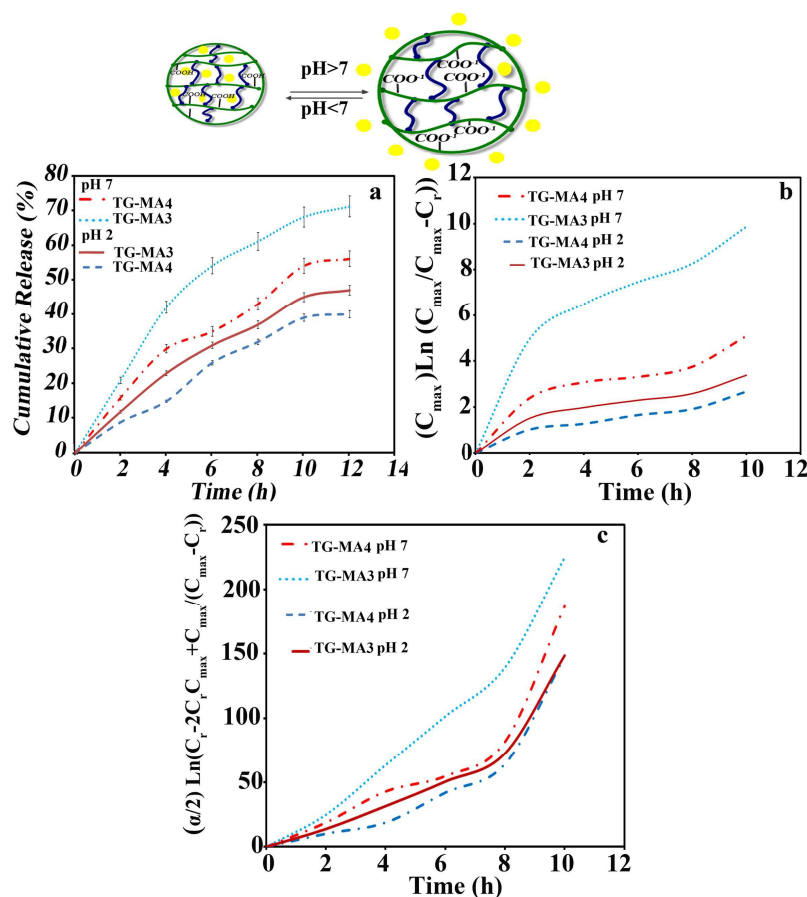
Fig. 7. *In vitro* release profiles of Quercetin-loaded TG-MA3 and TG-MA4 in PBS at pH 7 and pH 2 (a), experimental data for time-dependent release of Quercetin, plotted according to Eq. (6) (reversible first-order kinetics) (b), and Eq. (7) (reversible second-order kinetics) (c).

Table 2. Values of α, k_R, R^2 and $t_{1/2}$ for Quercetin released from TG-MA3 and TG-MA4

pH	Nanohydrogel	α	K_R	R^2(reversible first-order kinetics)	$t_{1/2}$	K_R	R^2(reversible second-order kinetics)
7	TG-MA3	2.44	21.485	0.9593	0.46717	0.8599	0.9722
7	TGMA4	1.27	16.197	0.8345	4.36	0.425	0.8796
2	TG-MA3	0.88	13.394	0.8787	0.89976	0.2921	0.9085
2	TGMA4	0.66	13.193	0.8234	1.3665	0.2345	0.9471

By comparing the R^2 values, it was observed that the *in vitro* drug release pattern of all formulations is in a good consistency with second-order kinetics. Defining the release kinetics as reversible second-order, the released drug half-time ($t_{1/2}$) may be determined through the Eq. (8), where $t_{1/2}$ is the necessary time for the concentration of drug in the solvent to reach 50% of C_{max}(maximum cumulative release), C_r is the cumulative release at a certain time and K_r is the kinetic constant. Table 2 describes the values of α, K_r, and $t_{1/2}$ for different composition of nanohydrogels at pH 2 and pH 7. Results showed that Quercetin was released faster from TG-MA3 nanohydrogel than TG-MA4. In the other word, TG-MA4 exhibited a higher $t_{1/2}$, which means that this nanohydrogel exhibited a lower rate and percentage release.

$$C_{max} \times Ln(C_{max}/C_{max}-C_r)=K_r\,t \qquad\qquad 6$$

$$\alpha/2 \times Ln((C_r-2C_rC_{max}+C_{max})/(C_{max}-C_r))= K_r\,t \qquad 7$$

$$t_{/2}= \alpha/2K_r \times Ln(3-2C_{max}) \qquad\qquad 8$$

Conclusions

Tragacanth gum (TG) was modified chemically with different amounts of glycidylmethacrylate (GMA) to obtain TG-GMAs. The cross-linking reaction in TG-GMAs was carried out via free radical polymerization in the presence of $K_2S_2O_8$ to form TG-MA

nanohydrogels. The nanohydrogels showed significant pH dependence, which had a considerable effect on their water absorption properties. The maximum swelling of nanohydrogels was 9.2 mg/mg at pH 7 after 6 h, and their average size has increased from ~80 nm at pH 2 to ~150 nm at pH 7. This was suggested to be due to the electrostatic repulsion among the ionized acid groups of TG which led to the expansion of nanohydrogels and increase in water uptake. The pH sensitivity of TG-MA nanohydrogels makes them a potential candidate for drug carrier. The drug loading capacity of the nanohydrogels increased with increasing the cross-linker content to a certain value. The maximum loading (EE=58%) was obtained for TG-MA3 at pH 7 after 2.5 h, and the average size of drug loaded nanohydrogels varied in the range of 142-168 nm. A relatively rapid release in the first 4 h followed by a sustained and slow release in the range of 55-70 % over a time period up to 12 h. TG-MA3 with maximum swelling at pH 7 also showed the highest release of 70 % after 12 h. According to the results, these natural gum based nanohydrogels may find great potential applications in biomedical arena and for oral drug delivery systems.

References

1. G. W. Ashley, J. Henise, R. Reid and D. V. Santi, *Proc. Natl. Acad. Sci*, 2013, **110**, 2318-2323.

2. F. Brandl, F. Kastner, R. M. Gschwind, T. Blunk, J. Teßmar and A. Göpferich, *J. Control. Release*, 2010, **142**, 221-228.

3. D. Schmaljohann, *Adv. Drug Deliv. Rev*, 2006, **58**, 1655-1670.

4. K. Hemmati, A. Masoumi and M. Ghaemy, *Polym.*, 2014, 49-56.

5. X. Sun, X. Zhao, L. Zhao, Q. Li, M. D'Ortenzio, B. Nguyen, X. Xu and Y. Wen, *J. Mater. Chem: B*, 2015.

6. X. Xie, D. Ma and L.-M. Zhang, *RSC Adv.*, 2015, **5**, 58746-58754.

7. Z. W. Low, P. L. Chee, D. Kai and X. J. Loh, *RSC Adv.*, 2015, **5**, 57678-57685.

8. Z.-S. Shen, X. Cui, R.-X. Hou, Q. Li, H.-X. Deng and J. Fu, *RSC Adv.*, 2015, **5**, 55640-55647.

9. B. S. Kaith, R. Jindal, H. Mittal and K. Kumar, *changes*, 2010, **25**, 27.

10. R. Zhang, M. Tang, A. Bowyer, R. Eisenthal and J. Hubble, *Biomater.*, 2005, **26**, 4677-4683.

11. S. Amin, S. Rajabnezhad and K. Kohli, *Sci. Res. Essays*, 2009, **4**, 1175-1183.

12. N. Bhattarai, J. Gunn and M. Zhang, *Adv. Drug Deliv. Rev*, 2010, **62**, 83-99.

13. N. Peppas, P. Bures, W. Leobandung and H. Ichikawa, *Eur. J. Pharm. Biopharm.*, 2000, **50**, 27-46.

14. N. Salamat-Miller, M. Chittchang and T. P. Johnston, *Adv. Drug Deliv. Rev*, 2005, **57**, 1666-1691.

15. K. Y. Lee and D. J. Mooney, *Chem. Rev.*, 2001, **101**, 1869-1880.

16. J. K. Tessmar and A. M. Göpferich, *Adv. Drug Deliv. Rev*, 2007, **59**, 274-291.

17. A. V. Reis, M. R. Guilherme, O. A. Cavalcanti, A. F. Rubira and E. C. Muniz, *Polym.*, 2006, **47**, 2023-2029.

18. K. Hemmati, A. Masoumi and M.Ghaemy, *Polym.*, 2015, 59, 49-56.

19. V. Rana, P. Rai, A. K. Tiwary, R. S. Singh, J. F. Kennedy and C. J. Knill, *Carbohydrate polymers*, 2011, 83(3), 1031-1047.

20. B. Singh and V. Sharma, *Carbohydrate polymers*, 2014, 101, 928-940.

21. M. Ghaemy and M. Naseri, *Carbohydrate polymers*, 2012, 90(3), 1265-1272.

22. J. N. BeMiller and R. L. Whistler, *Industrial gums: polysaccharides and their derivatives. Academic Press*, 2012.

23. M. Eastwood, W. Brydon and D. Anderson, *Toxicology letters, 1984, 21*(1), 73-81.

24. A. Masoumi and M. Ghaemy, *Carbohydrate Polymers,* 2014, 108, 206–215.

25. A. Barreto, V. Santiago, S. Mazzetto, J. Denardin, R. Lavín, G. Mele, M. Ribeiro, I. G. Vieira, T. Gonçalves, and N. Ricardo, *Journal of Nanoparticle Research,* 2011, *13*(12), 6545-6553.

26. A. Kumari, S. K. Yadav, Y. B. Pakade, B. Singh and S. C. Yadav, *Colloids and Surfaces B: Biointerfaces,* 2010, *80*(2), 184-192.

27. D. H. Lee, G. S. Sim, J. H. Kim, G. S. Lee, H. B. Pyo and B. C. Lee, *Journal of Pharmacy and Pharmacology,* 2007, *59*(12), 1611-1620.

28. L. Ferreira, M. Vidal, C. Geraldes and M. Gil, *Carbohydr. polym.*, 2000, **41**, 15-24.

29. W. van Dijk-Wolthuis, J. Kettenes-Van Den Bosch, A. Van der Kerk-Van Hoof and W. Hennink, *Macromolecules*, 1997, **30**, 3411-3413.

30. L. M. Meng, Y. C. Yuan, M. Z. Rong and M. Q. Zhang, *Journal of Materials Chemistry*, 2010, **20**, 6030-6038.

31. A. Parikh and D. Madamwar, *Bioresour. Technol.*, 2006, **97**, 1822-1827.

32. A. Kumar, M. Pandey, M. Koshy and S. A. Saraf, *Int. J. Drug. Deliv.*, 2011, **2**.

33. K. K. Rao and C.-S. Ha, *Polym. Bull.*, 2009, **62**, 167-181.

34. A. Thakur, R. Wanchoo and P. Singh, *Chem. Biochem. Eng. Q.*, 2011, **25**, 181-194.

35. H. Byun, B. Hong, S. Y. Nam, S. Y. Jung, J. W. Rhim, S. B. Lee and G. Y. Moon, *Macromol. Res.*, 2008, **16**, 189-193.

36. T. Tamura, N. Kawabata and M. Satoh, *Polym. Bull.*, 2000, **44**, 209-214.

37. M. C. I. M. Amin, N. Ahmad, N. Halib and I. Ahmad, *Carbohydr. polym.*, 2012, **88**, 465-473.

38. A. V. Reis, M. R. Guilherme, A. F. Rubira and E. C. Muniz, *J. Colloid Interface Sci.*, 2007, **310**, 128-135.

Captions

Fig. 1. Illustration of synthetic procedure for preparation of TG-MA nanohydrogels.

Fig. 2. FT-IR spectra of GMA (a), TG (b), TG-GMA (c), and TG-MA nanohydrogel(d).

Fig. 3. ^{1}H-NMR spectra of TG and TG-GMA recorded in D$_2$O and spectrum of GMA recorded in CDCl$_3$.

Fig. 4. SEM and TGA of TG and TG-MA3 nanohydrogel.

Fig. 5. The effect of cross-linker content (TG-MA1-TG-MA4) (a), solution pH (2.0-10.0) (b), immersion time (1-10 h) (c) and ionic strength (0.01-0.25 mg mL^{-1})(d) on the water uptake ratio (constant conditions: Temperature =25 ^{0}C, C$_0$ = 100 mg L^{-1}, ionic strength = 0.01mg mL^{-1}, pH 7, immersion time = 6 h, with varying the initial level of related factor).

Fig. 6. (a) Effect of GMA content on EE, (b) effect of time on EE at various concentrations of quercetin in TG-MA3, and (c) size of TGMA3 and TGMA4 nanohydrogels before and after loading at pH 7.

Fig. 7. *In vitro* release profiles of Quercetin-loaded TG-MA3 and TG-MA4 in PBS at pH 7 and pH2 (a), experimental data for time-dependent release of Quercetin, plotted according to Eq. (6) (reversible first-order kinetics) (b), and Eq. (7) (reversible second-order kinetics) (c).

Table 1. Starting materials in the preparation of nanohydrogels and gel fraction of them

Table 2. Values of α, K$_r$, R^2 and t $_{1/2}$ for Quercetin released from TG-MA3 and TG-MA4 nanohydrogels.